ACS chemical biology

Letters

pubs.acs.org/acschemicalbiology

Designed Phosphoprotein Recognition in *Escherichia coli*

Nicholas Sawyer,[†,‡] Brandon M. Gassaway,[∥,⊥] Adrian D. Haimovich,[⊥,#] Farren J. Isaacs,[⊥,#,‡] Jesse Rinehart,[∥,⊥] and Lynne Regan*[,†,‡,§]

[†]Department of Molecular Biophysics and Biochemistry, [‡]Integrated Graduate Program in Physical and Engineering Biology, [§]Department of Chemistry, [∥]Department of Cellular and Molecular Physiology, [⊥]Systems Biology Institute, and [#]Department of Molecular, Cellular, and Developmental Biology, Yale University, New Haven, Connecticut 06520, United States

Supporting Information

ABSTRACT: Protein phosphorylation is a central biological mechanism for cellular adaptation to environmental changes. Dysregulation of phosphorylation signaling is implicated in a wide variety of diseases. Thus, the ability to detect and quantify protein phosphorylation is highly desirable for both diagnostic and research applications. Here we present a general strategy for detecting phosphopeptide−protein interactions in *Escherichia coli*. We first redesign a model tetratricopeptide repeat (TPR) protein to recognize phosphoserine in a sequence-specific fashion and characterize the interaction with its target phosphopeptide *in vitro*. We then combine *in vivo* site-specific incorporation of phosphoserine with split mCherry assembly to observe the designed phosphopeptide−protein interaction specificity in *E. coli*. This *in vivo* strategy for detecting and characterizing phosphopeptide−protein interactions has numerous potential applications for the study of natural interactions and the design of novel ones.

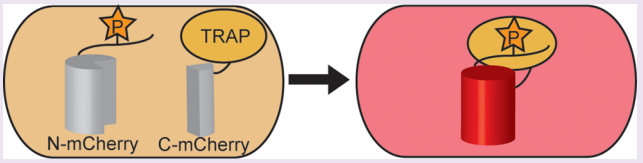

Post-translational modifications provide cells with an efficient mechanism for rapidly responding to external stimuli by reversibly modifying protein chemistry. Phosphorylation is one of the most common post-translational modifications and occurs with highest frequency on serine, threonine, and tyrosine residues. It is estimated that 65−80% of all protein phosphorylation occurs on serine residues.[1] Conversion of a hydroxyl group into a phosphate group significantly alters the local chemistry and may result in large-scale conformational changes and concomitant changes in the modified protein's activity.[2,3] Phosphorylation events are often further organized into cascades that can quickly amplify extracellular signals to trigger cellular remodeling.[4] Thus, the phosphorylation state of individual proteins in the proteome can provide a readout of a cell's metabolic and behavioral state.

A facile and efficient method for detecting site-specific serine phosphorylation in proteins is therefore highly desirable for both *in vitro* and *in vivo* applications. While phosphospecific antibodies and designed antibody fragments are powerful *in vitro* tools for Western blotting and immunofluorescence, critical structural disulfide bonds restrict their *in vivo* applications.[5,6] In addition, designed ankyrin repeat proteins (DARPins) have been selected to discriminate between phosphorylated and nonphosphorylated forms of extracellular signal-regulated kinase 2 (ERK2). However, this specificity is indirect, in that the DARPins recognize conformational changes in the kinase activation loop rather than the added phosphate group.[7]

Here we present a general strategy for detecting phosphopeptide−protein interactions in *E. coli* using split fluorescent protein assembly. Our approach was to first design and characterize a tetratricopeptide repeat affinity protein (TRAP) that distinguishes between phosphorylated and nonphosphorylated peptides in a sequence-specific fashion *in vitro*. We chose a structurally and thermodynamically well-characterized tetratricopeptide repeat (TPR) protein−peptide interaction as our design template.[8,9] In the TPR−peptide complex, the cognate MEEVD peptide is bound to the TPR in an extended conformation such that each peptide residue contributes to the TPR−peptide interaction affinity and specificity by interaction with a defined subset, or "pocket", of TPR residues.[10] Thus, TRAPs with novel binding specificity can be generated by mixing-and-matching TRAP pockets that have been selected to bind particular amino acids rather than performing new selections for every peptide target. This distributed mode of peptide recognition is not frequently observed in natural phosphopeptide-binding domains, which tend to recognize the phosphate group and one or two flanking amino acids specifically but not the entire peptide.[11] For *in vivo* applications, it is important to note that TPR proteins can be highly expressed in functional form in *E. coli*, yeast, and mammalian cytoplasm.

Because our goal is to distinguish between phosphorylated and nonphosphorylated forms of a target peptide, a key design feature for the TRAP was that interaction with the phosphate group should contribute significantly to the overall binding energy. Examination of the cocrystal structure of the parent TPR protein with its cognate MEEVD peptide[10] suggested a straightforward charge complementarity-based redesign in which a phosphoserine residue replaces the central glutamate

Received: May 27, 2014
Accepted: October 1, 2014
Published: October 1, 2014

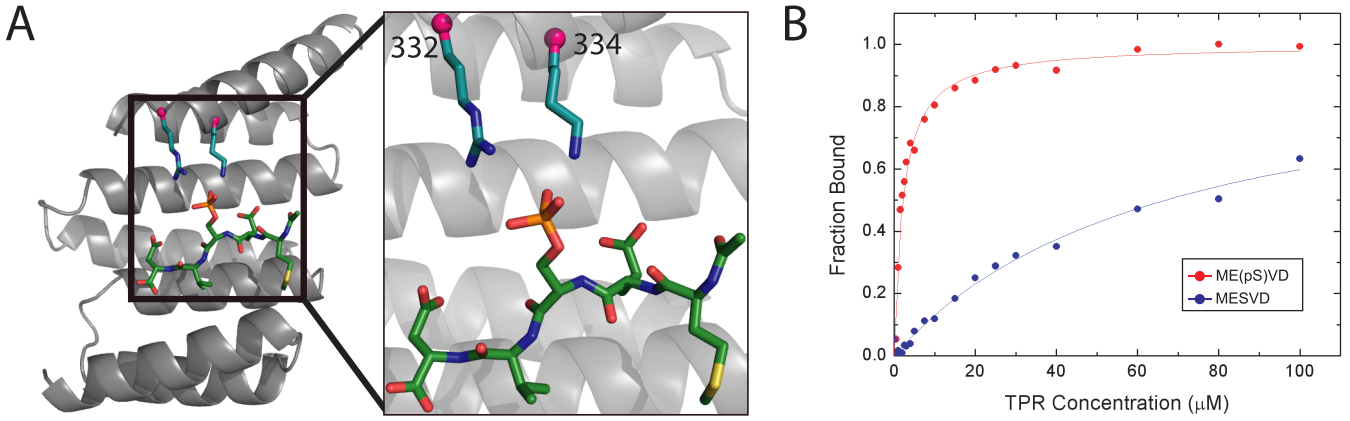

Figure 1. TRAP interaction with target phosphopeptide. (A) Model of the TRAP−phosphopeptide interaction. The entire TRAP−phosphopeptide complex is shown on the left with a zoomed-in view of the phosphopeptide binding region on the right. The TRAP protein backbone is depicted as a gray ribbon. The C_α of the phosphoserine binding pocket residues are shown as small pink spheres. Side chains for binding pocket residues (arginine at position 332 and lysine at position 334) are shown in stick representation with carbon atoms colored aqua. The phosphopeptide ME(pS)VD is shown as sticks with carbon atoms colored green. For both protein and phosphopeptide, nitrogen, oxygen, phosphorus, and sulfur atoms are colored blue, red, orange, and yellow, respectively. (B) TRAP binding to its phosphopeptide target and nonphosphopeptide analogue. Each data point shows the fraction of fluorescein-labeled peptide bound for a given TRAP concentration as measured by changes in the fluorescence anisotropy for the ME(pS)VD phosphopeptide (red) and MESVD peptide (blue). For each peptide, the solid lines show the fit of a 1:1 binding model, with dissociation constants of approximately 2 μM for the ME(pS)VD peptide and 67 μM for the MESVD peptide.

residue of the peptide and positively charged residues are introduced at nearby positions on the protein. We made and tested a set of TRAPs in which lysine and arginine are introduced combinatorially at positions 332 and 334 (numbering based on ref 10, PDB ID 1ELR). Figure 1A shows a model of such an interaction in which the phosphoserine side chain interacts with positively charged lysine and arginine residues introduced into the peptide binding pocket.

We measured the binding affinity of each TRAP for both the phosphorylated ME(pS)VD peptide and the nonphosphorylated MESVD peptide. Figure 1B shows binding curves for the interaction between each peptide and the most phosphospecific TRAP (i.e., shows the highest discrimination between the phosphorylated and nonphosphorylated peptides), as monitored by fluorescence anisotropy. Solid lines show fits to a simple 1:1 binding model. The extracted dissociation constants (K_ds) are approximately 2 μM for the ME(pS)VD phosphopeptide and 67 μM for the MESVD peptide at physiological ionic strength. The $\Delta\Delta G$ associated with binding the phosphate group is thus ∼2 kcal/mol. This interaction energy is significantly greater than the $\Delta\Delta G$ of ∼0.6 kcal/mol associated with the difference between MEAVD and MEEVD binding to the parent TPR2A protein.[8] This observation supports a model in which the TRAP interacts directly with the phosphate group. Other TRAPs exhibited similar binding affinities for the phosphorylated peptide but lower discrimination between the two peptides (i.e., higher affinities for the nonphosphorylated peptide, see Supplementary Table 1). For the most phosphospecific TRAP, a K_d of 67 μM for the MESVD peptide also indicates that the TRAP retains binding specificity for peptide residues flanking the phosphoserine residue. We used the most phosphospecific TRAP in subsequent experiments.

To detect TRAP−phosphopeptide interaction in *E. coli*, two components are required. The first is a system for site-specific incorporation of phosphoserine into any protein of interest.[12] The second is a method to detect interaction of the phosphoserine-containing peptide with a binding partner.

To site-specifically incorporate phosphoserine, we used amber codon suppression (Figure 2B), specifically the IPTG-inducible Sep-OTS in combination with an *E. coli* strain with partial UAG codon reassignment (EcAR7).[13] The Sep-OTS comprises an archaeal phosphoserine-tRNA synthetase (SepRS), a modified archaeal phosphoserine-tRNA ($tRNA^{Sep}$), and a phosphoserine-specific elongation factor (EF-Sep). The EcAR7 strain has three key modifications to the *E. coli* genome: (1) disruption of the *prfA* (release factor 1) gene to eliminate competition with the amber suppressor tRNA for UAG codons, (2) recoding of UAG stop codons for 7 essential genes to UAA to eliminate the deleterious effects of phosphoserine incorporation at these positions, and (3) a premature stop codon introduced into the *serB* serine phosphatase gene to reduce the intracellular hydrolysis of phosphoserine.

We combined the above with a newly developed pNAS duet system that allows independent coexpression of two proteins (e.g., target phosphopeptide and TRAP binding partner) from P_{BAD} and P_{LtetO} promoters[14,15] and has an origin of replication compatible with that of Sep-OTS (Figure 2A).

To confirm phosphoserine incorporation into our protein of interest at the desired position, we created glutathione-S-transferase (GST) fusion protein genes in which the peptide coding sequences for ME(pS)VD and MESVD are fused to GST by the same linker we use in subsequent split fluorescent protein studies. This strategy allows us to easily purify the GST fusion proteins for mass spectrometric analysis and avoid the challenges associated with purifying split fluorescent protein fragments.[16] We coexpressed the GST fusion proteins from the pNAS duet and the Sep-OTS in the EcAR7 strain, purified each fusion protein using glutathione resin, digested purified protein with trypsin, and performed mass spectrometric analysis of phosphoserine incorporation.

The LC−MS extracted ion chromatogram analyses for both GST fusion proteins are shown in Figure 2C. Ions with the mass-to-charge ratio (m/z) expected for the ME(pS)VD-containing phosphopeptide are only observed in the GST-ME(pS)VD sample. Similarly, ions with m/z expected for the MESVD-containing peptide are abundant in the GST-MESVD control sample with only small amounts observed in the GST-ME(pS)VD sample. These small amounts are likely a result of

dx.doi.org/10.1021/cb500658w | *ACS Chem. Biol.* 2014, 9, 2502−2507

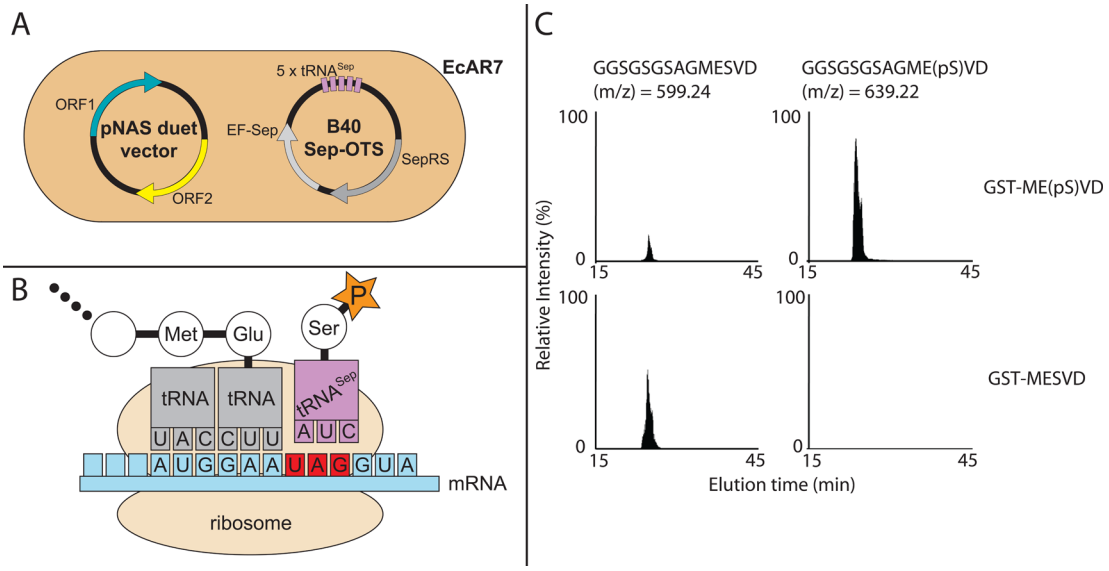

Figure 2. Confirmation of site-specific phosphoserine incorporation in pNAS duet/Sep-OTS coexpression system. (A) Schematic of coexpression using pNAS duet vector and Sep-OTS. Five copies of the phosphoserine-tRNA ($tRNA^{Sep}$, purple), the phosphoserine-specific tRNA synthetase (SepRS, dark gray), and the phosphoserine-specific elongation factor (EF-Sep, light gray) are coexpressed from the B40 Sep-OTS plasmid by induction with IPTG. Two additional proteins, such as the halves of split mCherry, can be expressed from the comaintained pNAS duet vector using two additional inducers (L-(+)-arabinose and anhydrotetracycline). (B) Schematic of phosphoserine incorporation by amber suppression. White circles with 3-letter amino acid abbreviations connected by thick black lines represent the growing polypeptide whose sequence is specified by the mRNA. $tRNA^{Sep}$ charged with phosphoserine (Ser + orange star indicating phosphate group) inserts phosphoserine in response to the amber (UAG) codon. (C) Mass spectrometric confirmation of site-specific phosphoserine incorporation into the target phosphopeptide sequence. Extracted ion chromatograms are shown for the indicated mass-to-charge ratios (corresponding to the indicated peptides) for two GST fusion proteins (GST-MESVD and GST-ME(pS)VD). The indicated phosphopeptide is only detected in the GST-ME(pS)VD sample. The control serine-containing peptide is most abundant in the GST-MESVD sample.

dephosphorylation during sample processing. Further mass spectrometry data are described in the Supporting Information.

Having established that phosphoserine is efficiently incorporated into the peptide sequence at the desired position, we next sought to detect the interaction of the phosphorylated peptide with the phosphospecific TRAP *in vivo* (Figure 3A). We expressed the phosphopeptide fused to the N-terminal half of mCherry (N-mCherry) and the phosphospecific TRAP fused to the C-terminal half of mCherry (C-mCherry). We and others have previously shown that fluorescence is reconstituted in split fluorescent protein systems only if the fusion partners interact.[16,17]

An increase in fluorescence over time is shown in Figure 3B for cells expressing the TRAP and phosphopeptide split mCherry fusion proteins (red bars). For comparison, the fluorescence is also shown for cells expressing split mCherry with either fused TRAP and nonphosphorylated peptide (blue bars) or a negative split mCherry control without fusion tags (gray bars). The fluorescence intensity increases most rapidly for the higher affinity TRAP–phosphopeptide pair. This faster increase in intensity is consistent with previous data that shows that, for a given interaction pair type (e.g., leucine zippers, TPR–peptide, etc.), fluorescence develops more quickly for higher affinity interactions.[16] The fluorescence of the TRAP-nonphosphopeptide pair is not surprising because this pair still interacts, albeit about 30-fold more weakly than the TRAP–phosphopeptide pair as measured *in vitro* (Figure 1B). Similar results were also observed in flow cytometry (Figure 3C) and with the same expression systems in an *E. coli* strain in which all genomic TAG stop codons were recoded to TAA stop codons (data not shown, strain based on ref 18).

The inset of Figure 3B shows the excitation and emission spectra for the TRAP–phosphopeptide pair (red), which are consistent with mCherry fluorescence despite a small shift in fluorescence excitation and emission maxima (590 and 602 nm, respectively) relative to published spectra for full-length mCherry.[19] Identical fluorescence spectra are also observed for the TRAP–nonphosphopeptide pair (data not shown), but there is no discernible fluorescence for the negative control (gray).

In conclusion, we have presented a system for the detection of phosphoprotein interactions in *E. coli*. The two key elements to our strategy are efficient site-specific incorporation of phosphoserine by amber suppression and detection of phosphopeptide–protein interaction using split mCherry assembly. In our proof-of-principle experiments, we show that this system can discriminate between phospho- and non-phospho-forms of a serine-containing peptide. The designed phosphospecific module we use to benchmark this system has a 30-fold difference in binding affinity between phospho- and nonphosphopeptides, which is significant but modest compared to many natural proteins.[20,21] Thus, we anticipate that our system will also work well for probing the binding specificity of natural phosphopeptide–protein interactions.

Several factors make this system attractive for future studies on phosphopeptide–protein interactions. First, the *in vivo* nature of the assay requires that the phosphopeptide–protein interaction is specific within the context of a cellular *milieu*. Using the Sep-OTS also eliminates the need to chemically synthesize phosphoserine-containing peptides or proteins, which is limited to short sequences and costs significantly more than synthesis of unmodified peptides. Further development of this approach as a high-throughput method has the

dx.doi.org/10.1021/cb500658w | *ACS Chem. Biol.* 2014, 9, 2502–2507

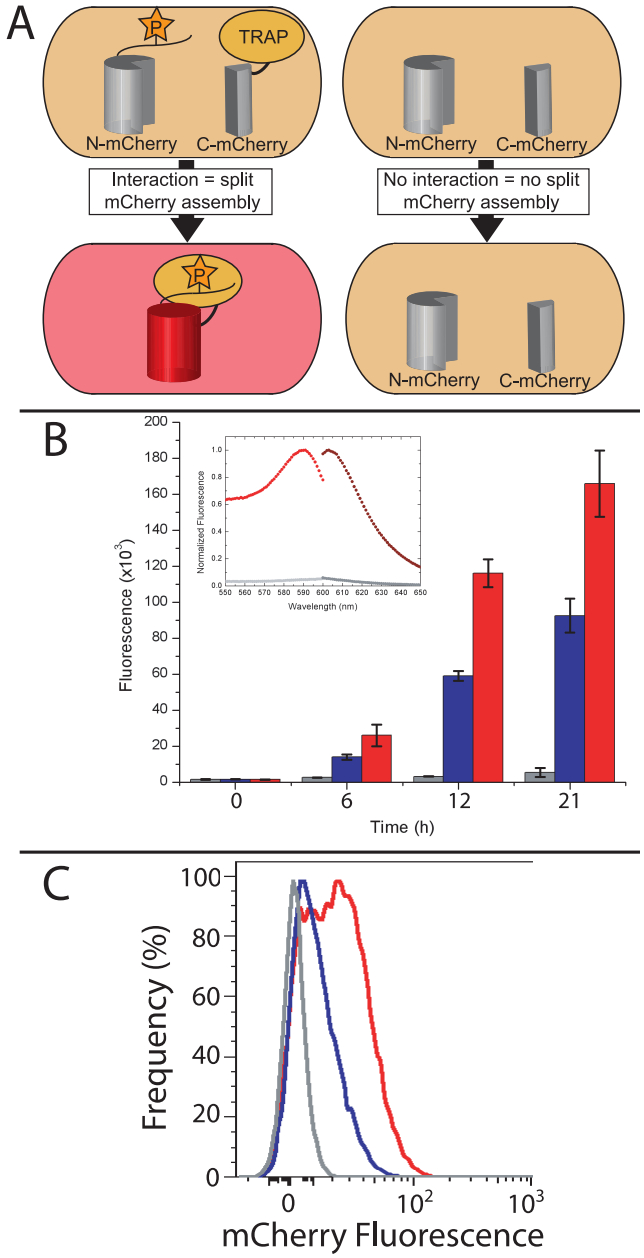

Figure 3. *In vivo* split mCherry assembly for TRAP−phosphopeptide interactions. (A) Schematic illustration of the *in vivo* split mCherry protein−peptide interaction assay. On the left, the N-terminal half of mCherry (N-mCherry) is fused to a phosphopeptide (phosphate group indicated by orange star). The C-terminal half of mCherry (C-mCherry) is fused to the TRAP binding partner. When the phosphopeptide and TRAP fusion proteins are coexpressed and interact, the halves of split mCherry are brought into close proximity, assemble, and fluoresce, producing a reddish cell. On the right, neither N-mCherry nor C-mCherry is fused to anything. Although they are coexpressed in the cell, they do not interact or assemble, and no red fluorescence is observed (i.e., the cell remains beige). (B) Time-dependent increase in fluorescence for *in vivo* split mCherry assembly. Bars show the fluorescence intensity of *E. coli* cell lysates prepared at the indicated time postinduction (excitation at 587 nm and emission at 610 nm). The results for three split mCherry pairs are shown: unfused N-mCherry + unfused C-mCherry (gray), N-mCherry fused to the MESVD peptide + C-mCherry fused to the TRAP (blue), and N-mCherry fused to the ME(pS)VD peptide + C-mCherry fused to the same TRAP (red). Error bars show the standard deviation for two or three biological replicates. The inset shows the excitation and emission spectra for reassembled mCherry for the phosphopeptide-TRAP pair (lighter red for excitation and darker red for emission). The peaks observed are consistent with mCherry fluorescence despite a small shift in excitation and emission maxima (590 and 602 nm, respectively.[19] Such peaks are absent from the spectra for the unfused N-mCherry + C-mCherry pair (lighter gray for excitation and darker gray for emission). (C) Flow cytometry measurements of *E.* coli cells containing different split mCherry pairs. Fluorescence histograms are shown for three split mCherry pairs: N-mCherry + C-mCherry (gray), N-mCherry fused to the MESVD peptide + C-mCherry fused to the TRAP (blue), and N-mCherry fused to the ME(pS)VD peptide + C-mCherry fused to the same TRAP (red). The mean fluorescence is 0.653 for N-mCherry + C-mCherry, 10.8 for N-mCherry fused to the MESVD peptide + C-mCherry fused to the TRAP, and 22.1 for N-mCherry fused to the ME(pS)VD peptide + C-mCherry fused to the same TRAP.

potential to provide a large collection of phosphopeptide-binding modules for detection and quantification of a wide variety of biological phosphopeptides. We envision that TRAPs with specificity for different biological phosphopeptides will be extremely useful for many applications such as Western blotting, affinity capture of phosphopeptides prior to mass spectrometric analysis, and immunofluorescence (when fused/conjugated to a fluorescent dye or protein).

For the study of protein−protein interactions more generally, the split mCherry duet vector, presented here as compatible with the Sep-OTS, is modular and can be easily modified by standard cloning techniques. Thus, the vector can facilitate the study of protein−protein interactions involving noncanonical amino acids that are introduced by other amber suppression systems.

METHODS

Detailed description of reagents, peptide synthesis, molecular cloning, protein expression and purification, and mass spectrometry sample preparation is provided in the Supporting Information.

Determination of TRAP-Peptide Dissociation Constants. Dissociation constants (K_ds) for each TRAP−peptide interaction were determined by fluorescence anisotropy using the fluorescein-labeled peptides described in the Supporting Information. Peptide and protein concentrations were separately determined by absorbance at 492 and 280 nm, respectively. For each measurement, the peptide concentration was held constant at 5 nM. For data fitting, the anisotropy of the peptide alone was subtracted from all measurements, and the adjusted data was fit in Origin 7.0 to a 1:1 binding model described by the equation below:

$$y = \frac{P_1 x}{P_2 + x}$$

where x is the protein concentration, y is the adjusted anisotropy, P_1 is the maximum anisotropy, and P_2 is the dissociation constant.

Strain and Plasmid Information. Phosphoprotein experiments were performed in the EcAR7 strain[13] and in a "completely recoded" strain (i.e., all genomic TAG codons recoded to TAA) derived from strain C321.ΔA.[18] Modifications to the strain C321.ΔA are (1) the tolC gene was integrated into the genome in place of the beta-lactamase gene to disrupt the *prfA* gene and permit use of plasmids with ampicillin resistance markers, and (2) a premature stop codon was introduced into the *serB* gene as in previous work.[12] The B40 Sep-OTS was prepared as described previously[22] except with 5 tandem copies of $tRNA^{Sep}$, which greatly enhances OTS activity (unpublished). The Sep-OTS plasmid and split fluorescent protein duets were

dx.doi.org/10.1021/cb500658w | *ACS Chem. Biol.* 2014, 9, 2502−2507

sequentially transformed into electrocompetent *E. coli* by electroporation.

Split mCherry Assembly Assay. Starter cultures were prepared by inoculating a single EcAR7 colony (transformed with both the Sep-OTS and a pNAS1B split fluorescent protein duet vector) into 5 mL of 2xYT supplemented with 100 μg/mL ampicillin and 25 μg/mL kanamycin. Starter cultures were grown for approximately 24 h at 30 °C with shaking at 250 rpm. For the assay, 1 mL of starter culture was inoculated into 100 mL of 2xYT media supplemented as above. Cells were grown at 30 °C with shaking at 250 rpm until OD_{600} reached 0.8 (4.5−5 h), at which point IPTG, phosphoserine, and anhydrotetracycline were added to final concentrations of 1 mM, 2 mM, and 100 ng/mL, respectively, to simultaneously induce expression of the Sep-OTS components and split mCherry fusion proteins as well as provide an enriched source of phosphoserine. Cultures were shifted to 20 °C for protein expression for an additional 6, 12, or 21 h with shaking at 250 rpm. Cells were harvested by centrifugation and stored at −80 °C.

Fluorescence Quantitation. Cell pellets were resuspended in 5 mL of lysis buffer (50 mM Tris pH 7.4, 300 mM NaCl, 1 mg mL^{-1} lysozyme, 5 mM β-mercaptoethanol, and 1 complete EDTA-free protease inhibitor tablet per 20 mL), incubated on ice for at least 1 h, sonicated, and centrifuged to remove insoluble material. Lysate fluorescence was measured using an excitation wavelength of 587 nm and an emission wavelength of 610 nm. Excitation scans from 550 to 600 nm were performed using an emission wavelength of 610 nm. Emissions scans from 600 to 650 nm were performed using an excitation wavelength of 587 nm.

Flow Cytometry. Fresh cell pellets were washed 4 times with 10 mL of phosphate-buffered saline (PBS) supplemented with 0.01% Tween-20 by resuspension and centrifugation (3000 rpm, 4 °C, 10 min). The final cell pellet was resuspended in 5 mL of the same buffer and diluted 100-fold in the same buffer. Sample fluorescence was analyzed on a Sony SY3200 instrument using a 100 μM nozzle, 532 nm laser for mCherry excitation, and 610/40 band-pass filter for mCherry emission.

■ ASSOCIATED CONTENT

Ⓢ Supporting Information

Detailed description of reagents, peptide synthesis, molecular cloning, protein expression and purification, and mass spectrometry sample preparation. This material is available free of charge via the Internet at http://pubs.acs.org.

■ AUTHOR INFORMATION

Corresponding Author

*E-mail: lynne.regan@yale.edu.

Notes

The authors declare no competing financial interest.

■ ACKNOWLEDGMENTS

We thank Cameron Godecke, Terrence Wu, and the West Campus Analytical Core for technical assistance. We thank Hans Aerni for helpful discussions about method development and data analysis. We thank the Regan laboratory for critical review of the manuscript. We thank the Raymond and Beverly Sackler Institute for Biological, Physical and Engineering Sciences for support. We acknowledge the following funding sources: NIH 5T32GM008283-24 (to N.S.), NIH MSTP-TG-T32GM07205 (to A.D.H.), Arnold & Mabel Beckman Foundation (to F.J.I.), DARPA contract N66001-12-C-4211 (to F.J.I. and J.R.), NIH NIDDK-K01DK089006 (to J.R.), and NSF DMR-1307712 (to L.R.).

■ REFERENCES

(1) Khoury, G. A., Baliban, R. C., and Floudas, C. A. (2011) Proteome-wide post-translational modification statistics: frequency analysis and curation of the swiss-prot database. *Sci. Rep. 1*, 90.

(2) Canagarajah, B. J., Khokhlatchev, A., Cobb, M. H., and Goldsmith, E. J. (1997) Activation mechanism of the MAP kinase ERK2 by dual phosphorylation. *Cell 90*, 859−869.

(3) Stoothoff, W. H., and Johnson, G. V. W. (2005) Tau phosphorylation: physiological and pathological consequences. *Biochim. Biophys. Acta 1739*, 280−297.

(4) Dhillon, A. S., Hagan, S., Rath, O., and Kolch, W. (2007) MAP kinase signalling pathways in cancer. *Oncogene 26*, 3279−3290.

(5) Nairn, A. C., Detre, J. A., Casnellie, J. E., and Greengard, P. (1982) Serum antibodies that distinguish between the phospho- and dephospho-forms of a phosphoprotein. *Nature 299*, 734−736.

(6) Koerber, J. T., Thomsen, N. D., Hannigan, B. T., DeGrado, W. F., and Wells, J. A. (2013) Nature-inspired design of motif-specific antibody scaffolds. *Nat. Biotechnol. 31*, 916−921.

(7) Kummer, L., Parizek, P., Rube, P., Millgramm, B., Prinz, A., Mittl, P. R. E., Kaufholz, M., Zimmermann, B., Herberg, F. W., and Plückthun, A. (2012) Structural and functional analysis of phosphorylation-specific binders of the kinase ERK from designed ankyrin repeat protein libraries. *Proc. Natl. Acad. Sci. U.S.A. 109*, E2248−E2257.

(8) Brinker, A., Scheufler, C., von der Mülbe, F., Fleckenstein, B., Herrmann, C., Jung, G., Moarefi, I., and Hartl, F. U. (2002) Ligand discrimination by TPR domains: Relevance and selectivity of EEVD-recognition in Hsp70·Hop·Hsp90 complexes. *J. Biol. Chem. 277*, 19265−19275.

(9) Kajander, T., Sachs, J. N., Goldman, A., and Regan, L. (2009) Electrostatic interactions of Hsp-organizing protein tetratricopeptide domains with Hsp70 and Hsp90: computational analysis and protein engineering. *J. Biol. Chem. 284*, 25364−25374.

(10) Scheufler, C., Brinker, A., Bourenkov, G., Pegoraro, S., Moroder, L., Bartunik, H., Hartl, F. U., and Moarefi, I. (2000) Structure of TPR domain-peptide complexes: Critical elements in the assembly of the Hsp70-Hsp90 multichaperone machine. *Cell 101*, 199−210.

(11) Yaffe, M. B., and Elia, A. E. H. (2001) Phosphoserine/threonine-binding domains. *Curr. Opin. Cell Biol. 13*, 131−138.

(12) Park, H.-S., Hohn, M. J., Umehara, T., Guo, L.-T., Osborne, E. M., Benner, J., Noren, C. J., Rinehart, J., and Söll, D. (2011) Expanding the genetic code of *Escherichia coli* with phosphoserine. *Science 333*, 1151−1154.

(13) Heinemann, I. U., Rovner, A. J., Aerni, H. R., Rogulina, S., Cheng, L., Olds, W., Fischer, J. T., Söll, D., Isaacs, F. J., and Rinehart, J. (2012) Enhanced phosphoserine insertion during *Escherichia coli* protein synthesis via partial UAG codon reassignment and release factor 1 deletion. *FEBS Lett. 586*, 3716−3722.

(14) Smith, B. R., and Schleif, R. (1978) Nucleotide sequence of the L-arabinose regulatory region of *Escherichia coli* K12. *J. Biol. Chem. 253*, 6931−6933.

(15) Lutz, R., and Bujard, H. (1997) Independent and tight regulation of transcriptional units in *Escherichia coli* via the LacR/O, the TetR/O and AraC/I_1-I_2 regulatory elements. *Nucleic Acids Res. 25*, 1203−1210.

(16) Magliery, T. J., Wilson, C. G. M., Pan, W., Mishler, D., Ghosh, I., Hamilton, A. D., and Regan, L. (2005) Detecting protein-protein interactions with a green fluorescent protein fragment reassembly trap: Scope and mechanism. *J. Am. Chem. Soc. 127*, 146−157.

(17) Fan, J. Y., Cui, Z. Q., Wei, H. P., Zhang, Z. P., Zhou, Y. F., Wang, Y. P., and Zhang, X. E. (2008) Split mCherry as a new red bimolecular fluorescence complementation system for visualizing protein-protein interactions in living cells. *Biochem. Biophys. Res. Commun. 367*, 47−53.

(18) Lajoie, M. J., Rovner, A. J., Goodman, D. B., Aerni, H. R., Haimovich, A. D., Kuznetsov, G., Mercer, J. A., Wang, H. H., Carr, P. A., Mosberg, J. A., Rohland, N., Schultz, P. G., Jacobson, J. M., Rinehart, J., Church, G. M., and Isaacs, F. J. (2013) Genomically recoded organisms expand biological functions. *Science 342*, 357−360.

(19) Shaner, N. C., Campbell, R. E., Steinbach, P. A., Giepmans, B. N. G., Palmer, A. E., and Tsien, R. Y. (2004) Improved monomeric red, orange, and yellow fluorescent proteins derived from *Discosoma* sp. red fluorescent protein. *Nat. Biotechnol. 22*, 1567−1572.
(20) Yaffe, M. B., Rittinger, K., Volinia, S., Caron, P. R., Aitken, A., Leffers, H., Gamblin, S. J., Smerdon, S. J., and Cantley, L. C. (1997) The structural basis for 14-3-3:phosphopeptide binding specificity. *Cell 91*, 961−971.
(21) Verdecia, M. A., Bowman, M. E., Lu, K. P., Hunter, T., and Noel, J. P. (2000) Structural basis for phosphoserine-proline recognition by group IV WW domains. *Nat. Struct. Biol. 7*, 639−643.
(22) Steinfeld, J. B., Aerni, H. R., Rogulina, S., Liu, Y., and Rinehart, J. (2014) Expanded cellular amino acid pools containing phosphoserine, phosphothreonine, and phosphotyrosine. *ACS Chem. Biol. 9*, 1104−1112.